Int. J. Electrochem. Sci., 8 **(2013)** 2140 - 2153

International Journal of
ELECTROCHEMICAL
SCIENCE
www.electrochemsci.org

Green Inhibitors for Copper Corrosion by Mangrove Tannin

A. M. Shah[1], *A. A. Rahim*[1,*], *S. A. Hamid*[2] *and S. Yahya*[1]

[1] School of Chemical Sciences, Universiti Sains Malaysia, Penang, Malaysia
[2] Kulliyah Of Science, International Islamic University Malaysia, Jalan Istana, Bandar Indera Mahkota, Kuantan, Pahang Malaysia
[*]E-mail: afidah@usm.my

Received: 8 August 2012 / *Accepted:* 27 November 2012 / *Published:* 1 February 2013

Inhibition of copper corrosion by mangrove tannin has been investigated in aqueous 0.5 M hydrochloric acid solution using weight loss method, potentiodynamic polarization, electrochemical impedance spectroscopy (EIS), scanning electron microscopy (SEM) along with energy dispersive (EDX), atomic absorption spectroscopy (AAS) and ion chromatography (IC). Inhibition efficiency of 82 % was achieved with the addition of 3.0 g L^{-1} mangrove tannin from potentiodynamic polarisation measurements. Potentiodynamic curves showed that the presence of mangrove tannin in 0.5 M hydrochloric acid solution predominantly affected the cathodic process, decreased the corrosion current density and shifted the corrosion potential towards more negative values. Results obtained from the gravimetric (weight loss), potentiodynamic polarisation and impedance measurements showed similar trends of inhibition efficiency. AAS and IC analysis results showed that the concentrations of copper (II) ions and chloride ions in the electrolyte solutions decreased and increased, respectively, after the corrosion process, when the concentrations of mangrove tannin increased. Adsorption of mangrove tannin on the copper surface in 0.5 M hydrochloric acid solution fitted well with the Langmuir adsorption isotherm model. A change of morphology was observed after the addition of mangrove tannin as shown from SEM analysis.

Keywords: Copper, Corrosion, Inhibitor, Electrochemical impedance spectroscopy (EIS), Electrochemistry

1. INTRODUCTION

An excellent thermal conductivity, good corrosion resistance and mechanical workability are physical properties for copper that explain the wide applications of copper and its alloys in different industries. However, most of the industrial processes lead to corrosion problems. Copper generally corrodes when it is exposed to ammonia, oxygen, or fluids with high sulfur content. Another source of copper corrosion is the presence of anions in the environment such as chlorides, sulfates, and

bicarbonates. In industries, hydrochloric acid is extensively used for acid pickling, acid cleaning and removal of rust and acid de-scaling processes [1]. Consequently, the control of the corrosion processes under the influence of acidic condition and the presence of chloride ions are important subjects worthy of intensive investigations.

One of the most important and practical methods in the corrosion protection of metals is the use of organic inhibitors to protect the metal surface from the corrosion environment, especially in aggressive media [1, 2]. Generally organic compounds containing heteroatoms such as oxygen, nitrogen or sulphur, behaves fairly well as a corrosion inhibitor in acidic media [3]. The strength of the coordination bonds of heteroatom (O < N < S < P) parallels its efficiency as corrosion inhibitors.

Due to the currently imposed environmental requirements for eco-friendly corrosion inhibitors, there is a growing interest in the use of natural products such as leaves, seeds or bark extracts. Some papers have reported the use of natural products in the development of effective green corrosion inhibitors for different metals in various environments [4-22]. Tannins are a class of non-toxic biodegradable organic compounds. They are polyphenols of vegetal origin extracted usually from the bark of trees such as the quebracho, mimosa, chestnut and mangrove. The basic components of tannins are sugars, gallic acid, ellagic acid, and flavanoids [12]. These compounds are subdivided into condensed and hydrolysable tannins [23]. Mangrove is of the condensed type that are also known as proanthocyanidins (PAs), consisting of mainly polymers of flavanoids [24]. Previous research reported that vegetal tannin extracted from Takaot galls (*Tamarix articulata*) can be used as anodic inhibitors for copper corrosion [12]. It has also been found that mangrove, mimosa and quebracho tannins are very good inhibitors for mild steel corrosion [25, 26]. Due to the vicinity of the hydroxyl groups on the aromatic rings, tannins are able to form chelates with metallic cations and it is very important for anti-corrosion activities, because 'site-specific scavenging' may occur [27]. Hence, the tannins extract is expected to have excellent ability for inhibitory action through oxygen active centres. In this study, the potential of mangrove tannin extracted from the bark, a waste product of the charcoal industry as copper corrosion inhibitors in 0.5 M hydrochloric acid were investigated.

2. EXPERIMENTAL

2.1 Extraction of tannins

Mangrove bark samples, which were obtained from Matang Forest, Malaysia, were ground and 25 g of the powder was extracted by total immersion in 500 mL of 70 % aqueous acetone for 72 h at room temperature (30 °C). The extracts were evapourated using rotary evapourator at 40 °C to remove the acetone and finally the residue was freeze-dried to produce the mangrove tannin (MT) [26].

2.2 Gravimetric methods

The copper specimens of size 10 mm x 10 mm x 0.3 mm for weight loss measurements were polished using different grades of abrasive paper from 400 up to 1000, washed with distilled water,

degreased with acetone and dried before immersing into the test solution. The experiment was carried out in a test tube containing 10 mL test solution. After 24 h of immersion in 0.5 M hydrochloric acid solution with and without the addition of MT at different concentrations, the specimen was withdrawn, rinsed with distilled water, washed with acetone, dried and weighed. Three measurements were performed in each case. The percentage of inhibition efficiency (*IE*) was calculated as follows:

$$IE = \left(1 - \frac{W_{(i)}}{W_{(o)}}\right) \times 100 \qquad (1)$$

Where, W_o - weight loss of copper without inhibitor and W_i - weight loss of copper with inhibitor.

2.3 Electrochemical measurements

A conventional three-electrode cell, employing a copper disc (99.9% pure) as working electrode (WE), platinum as counter electrode, and saturated calomel electrode as reference electrode (SCE) were used for measurements. The WE was polished using different grades of abrasive paper ranging from 400 to 1000, washed with distilled water, degreased with acetone and finally thoroughly rinsed with distilled water before immersing into the test solution with an exposed area of 3.142 cm^2. The measurements were performed in 0.5 M hydrochloric acid solution with and without the addition of different inhibitor concentrations in an aerated environment. The polarisation curves were recorded by using Voltalab 21 model PGP201 potentiostat-galvanostat, equipped with VoltaMaster 4 software for data analysis. The working electrode was immersed into the test solution for 15 min to establish a steady state open circuit potential (E_{corr}). The potentiodynamic polarisation experiments were conducted at a scan rate of 1 mV s^{-1} in the potential range ±300 mV relative to corrosion potential (E_{corr}). The percentage of inhibition efficiency (*IE)* was calculated from the I_{corr} values by:

$$IE = \left(1 - \frac{I_{corr(i)}}{I_{corr(o)}}\right) \times 100 \qquad (2)$$

Where, $I_{corr(i)}$ and $I_{corr(o)}$ are the inhibited and uninhibited corrosion current densities, respectively. The I_{corr} was obtained by extrapolating the anodic and cathodic curves of the Tafel plot towards E_{corr}.

For all electrochemical impedance spectroscopy (EIS), the measurements were carried out using Gamry Reference 600. The excitation amplitude of 10 mV peak-to-peak in the frequency range from 0.05 Hz to 100 kHz, at 30 min open circuit potential, was used. The percentage of inhibition efficiency, *IE*, was calculated from the R_{ct} values by:

$$IE = \left(1 - \frac{R_{ct(o)}}{R_{ct(i)}}\right) \times 100 \qquad (3)$$

Where, $R_{ct(o)}$ is the charge transfer resistance of the metal in inhibitor free solution and $R_{ct(i)}$ is its value in the presence of the inhibitor.

2.4 Scanning electron microscopy (SEM) analysis

Surface analysis was conducted on the copper substrate from the electrochemical experiments. After the weight loss method, copper substrates in the presence and the absence of MT in 0.5 M hydrochloric acid were cleaned, slowly rinsed with distilled water and dried. The analysis was performed using SEM LEO SUPRA 50VP.

2.5 Adsorption atomic spectroscopy (AAS) analysis

Atomic adsorption analysis was conducted by using atomic adsorption spectrometer model AAnalyst 200 Perkin Elmer to determine the concentration of copper(II) ions in 0.5 M hydrochloric acid after gravimetric and potentiodynamic measurements. The calibration curve of copper(II) ions was constructed drawn before analysing the electrolyte solution. All samples containing copper ions were diluted with ultra pure water to ensure that the concentration of metal ions are within the range of the calibration curve.

2.6 Ion chromatography (IC) analysis

Ion chromatography analysis has been carried out to determine the concentration of chloride ions in 0.5 M hydrochloric acid solution after gravimetric and potentiodynamic tests. The analysis was performed using ion chromatography Metrohm 792 Basic IC equipped with a capillary column Metrosep Asupp 5-150 (size 4.0 x 150 mm) with capacity of 5.0 μm particle size. Flow rate was set at 0.7 mL min^{-1} with a temperature of 20.0 º C and pressure of 7.1 MPa. All samples containing chloride were diluted with ultra pure water to reduce the concentration of chloride ions. The sample solutions were injected into the colums using a syringe equipped with a 0.45 μm filter.

3. RESULTS AND DISCUSSION

3.1 Gravimetric methods

Figure 1 shows the graph of % IE in the addition of MT. The graph shows a sharp increment of % IE from 0.1 to 1.0 g L^{-1} MT followed by a gradual increase from 1.0 to 3.0 g L^{-1} MT. The IE in the presence of MT increased up to 72.8 % at 3 g L^{-1}. Corrosion rates (R_{corr}) of copper were calculated by considering the total area of sample and immersion times, which is expressed in mg cm^{-2} h^{-1}. The data from Table 1 reveals that R_{corr} of copper in 0.5 M hydrochloric acid is 30.2 x 10^{-2} mg cm^{-2} h^{-1} and subsequently decreased to 8.2 x 10^{-2} mg cm^{-2} h^{-1} with the addition of MT.

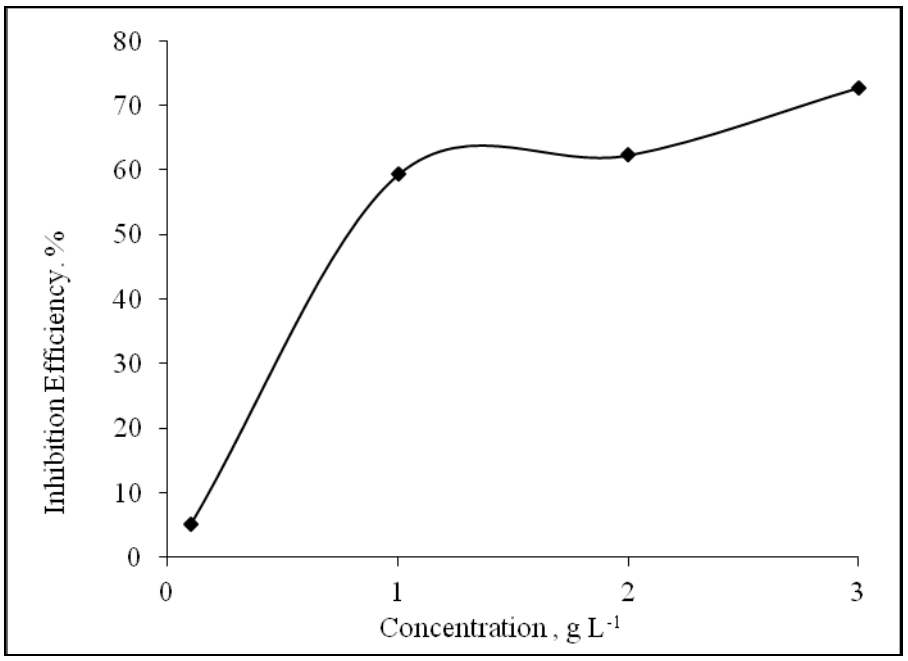

Figure 1. Graph of IE obtained from weight loss measurements in the presence of MT in 0.5 M hydrochloric acid

Table 1. Inhibition efficiency for various concentrations of MT for the corrosion of copper in 0.5 M hydrochloric acid obtained from weight loss measurements

Concentration (g L^{-1})	R_{corr} (mg cm^{-2} h^{-1}) x 10^{-2}	IE (%)
0.5 M hydrochloric acid	30.2	-
MT		
0.1	28.7	5.0
1.0	12.3	59.3
2.0	11.4	62.3
3.0	8.2	72.8

3.2 Electrochemical measurements

3.2.1 Potentiodynamic polarisation measurements

Figure 2 illustrates the anodic and cathodic polarisation curves of copper in the absence and the presence MT in 0.5 M hydrochloric acid solution. The mechanism of anodic dissolution of copper in acidic solution is as follows [28]:

$$Cu + Cl^- \leftrightarrow CuCl_{ads} + e^- \quad (4)$$

$$CuCl_{ads} + Cl^- \leftrightarrow CuCl_2^- + e^- \quad (5)$$

The cathodic corrosion reaction in an aerated acidic solution is:

$$4H^+ + O_2 + 4e^- \leftrightarrow 2H_2O \qquad (6)$$

The polarisation curve for copper in chloride media shows the passive transition region (A) that is attributed to the formation of a CuCl film arising from the lateral growth and thickening of CuCl nuclei [2]. In addition, the corrosion potentials of the polarisation curves are shifted towards more negative potentials in the presence of MT due to the decrease in the rate of the cathodic reaction. It was also observed that the presence of MT predominantly affected the cathodic parts of the curves (Figure 2). Since the transfer of oxygen from the bulk solution to the copper/solution interface will strongly affect the rate of oxygen reduction according to the reaction of equation (6), it can be inferred that the adsorbed layer behaves as a cathodic inhibitor to copper corrosion by retarding the O_2 diffusion to the cathodic sites of the copper surface. This indicates that MT cathodically inhibits the corrosion process of the copper, and the ability of MT as corrosion inhibitors are enhanced as the concentrations are increased.

Table 2 represents the values of E_{corr}, I_{corr} and IE obtained from Figure 2. From this Table, it is clear that the presence of MT decreased the I_{corr} values. The decrease in I_{corr} value by increasing tannins concentration is probably due to the decreases in the aggressive ions (Cl^-) attack on the copper surface due to the adsorption of the inhibitor molecules as confirmed by the SEM-EDX analysis.

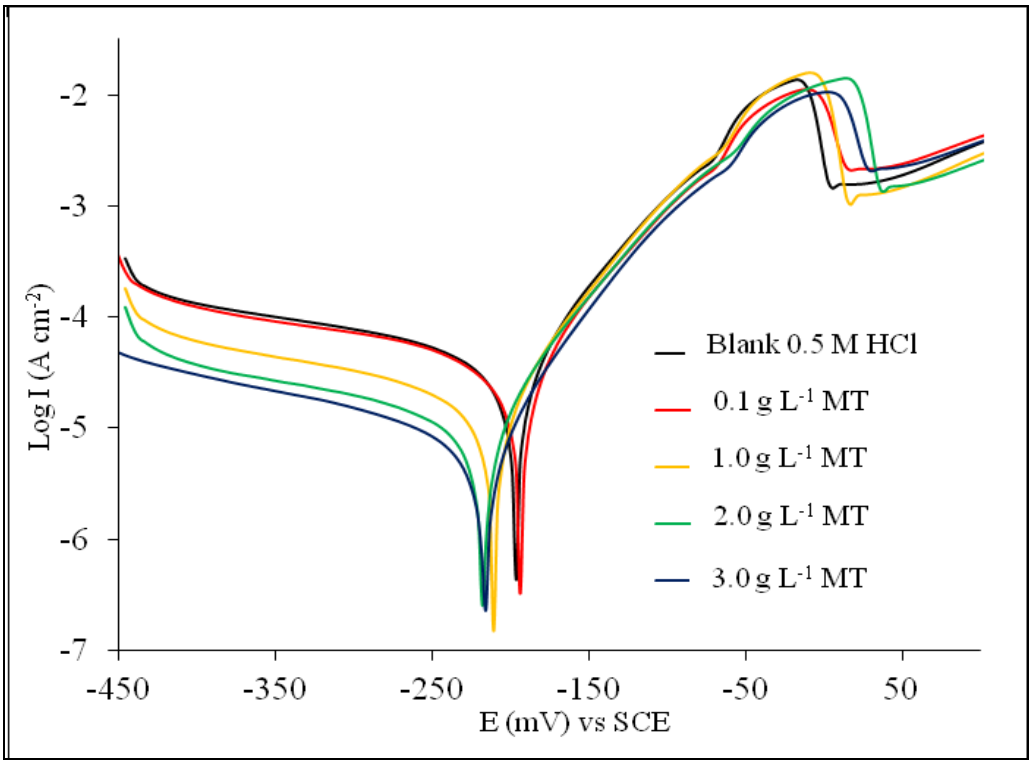

Figure 2. Potentiodynamic curves of copper containing different concentrations of MT in 0.5 M hydrochloric acid

Table 2. Corrosion parameters obtained from the Tafel analysis of the polarisation curves.

Concentration	MT		
	E_{corr} (mV)	I_{corr} (□A cm^{-2})	IE %
Blank 0.5 M hydrochloric acid	-196.5	26.1	-
0.1 g L^{-1}	-193.6	22.0	15.7
1.0 g L^{-1}	-219.1	7.7	70.5
2.0 g L^{-1}	-217.7	6.6	74.7
3.0 g L^{-1}	-214.6	4.6	82.4

3.2.2 Electrochemical impedance spectroscopy (EIS)

EIS measurements were carried out to determine the kinetic parameters for electron transfer reactions at the copper/electrolyte interface and simultaneously about the surface properties of the investigated system and the shape of the impedance diagram will provide mechanistic information. The Nyquist impedance plots obtained for copper electrode in the absence and presence of MT in 0.5 M hydrochloric acid solution are shown in Figure 3.

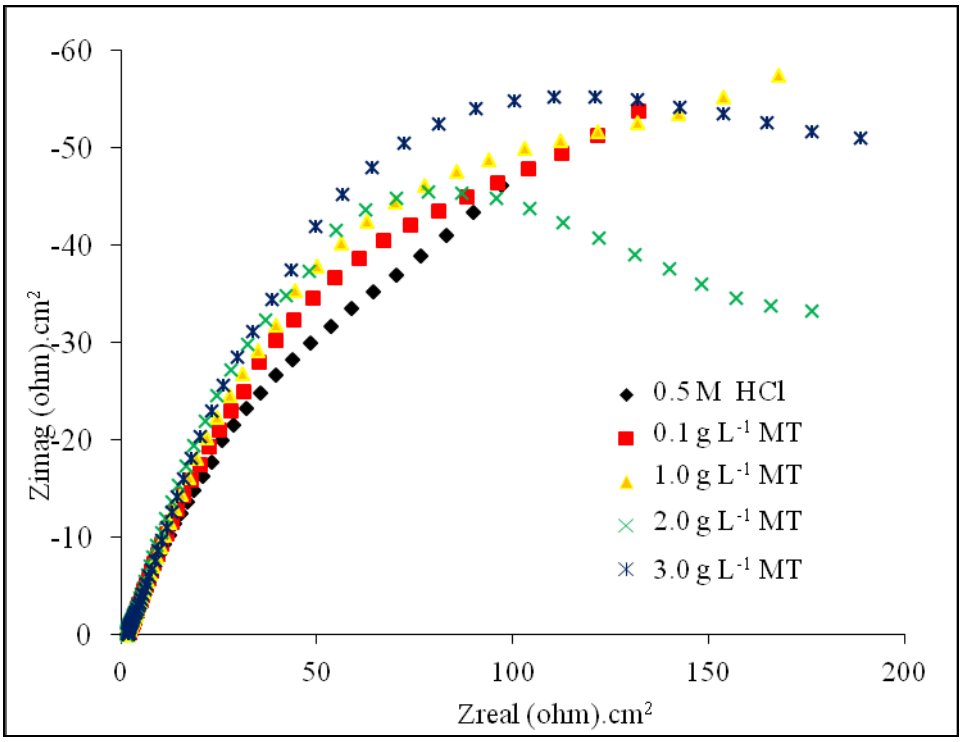

Figure 3. Nyquist plots for copper in 0.5 M hydrochloric acid in the absence and presence of different concentrations of MT

The Nyquist plots show a depressed semicircular with their centers below the real axis. This phenomenon that is known as the frequency dispersion effect is typical for solid metal electrodes [29].

The similar electrochemical behavior between uninhibited and inhibited solution suggests that both conditions have an active corrosion phenomenon under acid environments. The impedance data points of the copper electrode in the presence of different inhibitor concentrations were analyzed using the equivalent circuit shown in Figure 4. This equivalent circuit which has been previously reported [29], fitted well with our experimental results. The calculated equivalent circuit consists of the ohmic resistances of the corrosion product films and the solution enclosed between the working electrode and the reference electrode, R_s, the charge-transfer resistance represented by R_{ct}, where the values signify the electron transfer across the surface and is inversely proportional to corrosion rate. The constant phase element (CPE) is substituted for the capacitive element to give a more accurate fit [30]. The calculated equivalent circuit parameters for Cu in acidic chloride solutions containing different concentrations of both tannins are presented in Table 3. The CPE is a special element whose admittance value is a function of angular frequency (ω), and the phase is independent of the frequency. The admittance and impedance are, respectively, expressed as:

$$Y_{CPE} = Y_0 (j\omega)^n \quad (7)$$

and

$$Z_{CPE} = \left(\frac{1}{Y_0}\right)\left[(j\omega)^n\right]^{-1} \quad (8)$$

where the Y_0 is the magnitude of the CPE, j is the imaginary number ($j^2 = -1$), α is the phase angle of the CPE and $n = \alpha/(\pi/2)$. Values of α are usually related to the roughness of the electrode surface. The smaller the value of α, the higher the surface roughness [30, 31]. The first CPE_{dl}, with its n_1 close to 1.0 represent double layer capacitors with porous structures on the surface. The second CPE_{ads}, with its n_2 around 0.50, reveals the presence of a diffusion process at the interfacial layer [29] and also suggests that the adsorbed tannin layer on the copper surface blocks the mass transport of the aggressive ion (Cl^-) onto the copper surface and acts like a resistor [32]. The % IE values increased upon addition of MT and the effect is enhanced when the tannin concentrations are increased (Table 3), which is in good agreement with results obtained by the weight loss and potentiodynamic polarisation methods (Table 1 and 2). Maximum % IE of 87.6 % was obtained for MT.

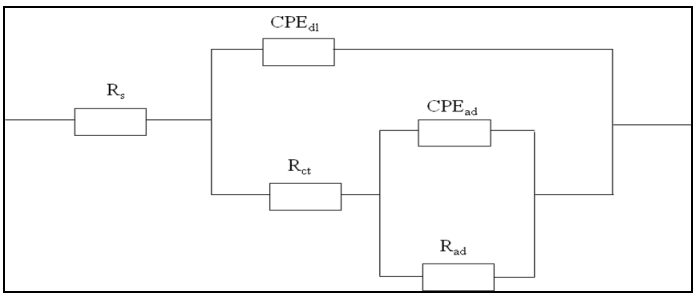

Figure 4. The electrochemical equivalent circuit used to fit the impedance spectra

Table 3. Values of the elements of equivalent circuit in Figure 4 required for fitting the EIS for copper in 0.5 M hydrochloric acid in the presence of MT.

C_{sol}	R_s (Ωcm^2)	R_{ct} ($k\Omega cm^2$)	CPE_{dl} ($\mu F cm^{-2}$)	n_1	R_{ads} ($k\Omega cm^2$)	CPE_{ads} ($mF cm^{-2}$)	n_2	IE %
0.5 M hydrochloric acid	5.56	0.115	15.8	0.82	0.59	3.38	0.49	-
MT								
0.1 g L^{-1}	6.44	0.22	93.4	0.84	0.70	2.31	0.52	47.2
1.0 g L^{-1}	6.06	0.31	15.2	1.00	0.73	1.71	0.56	62.8
2.0 g L^{-1}	5.05	0.70	41.7	0.91	0.57	1.09	0.62	83.3
3.0 g L^{-1}	5.57	0.93	66.8	0.87	0.73	1.33	0.59	87.6

3.3 The adsorption isotherm

Since the potentiodynamic and EIS measurements show a positive correlation between the concentration of MT and the inhibition efficiency of copper in 0.5 M hydrochloric acid solution, the adsorption behaviour of MT on the metal surface was studied to explain the nature of metal inhibitor interactions [19]. The adsorption process that is directly related to IE and the surface coverage, (θ) was calculated using the equation below [33]:

$$\theta = \frac{IE}{100} \qquad (9)$$

The Frumkin, Temkin and Langmuir adsorption isotherm models were tested by fitting the data from both methods. The additions of MT in 0.5 M hydrochloric acid were found to obey the Langmuir adsorption isotherm model according to the following equation:

$$\frac{\theta}{1-\theta} = KC \qquad (10)$$

Where, C is the concentration of the inhibitor, θ is the degree of surface coverage and K is the adsorption equilibrium constant. The Langmuir adsorption isotherm is rearranged and the following equation is obtained:

$$\frac{C}{\theta} = \frac{1}{K} + C \qquad (11)$$

The K value is related to the Gibbs free energy of adsorption, $\Delta G°_{ads}$, according to the following equation:

$$K = \frac{1}{C_{solvent}} \exp\left(\frac{-\Delta G_{ads}^{o}}{RT}\right) \quad (12)$$

Where, R is gas constant (8.314 J K^{-1} mol^{-1}), T is absolute temperature (room temperature 303 K) , $\Delta G°_{ads}$ is Gibbs free energy of adsorption and $C_{solvent}$ is the concentration of water that is equal to 999 g L^{-1}.

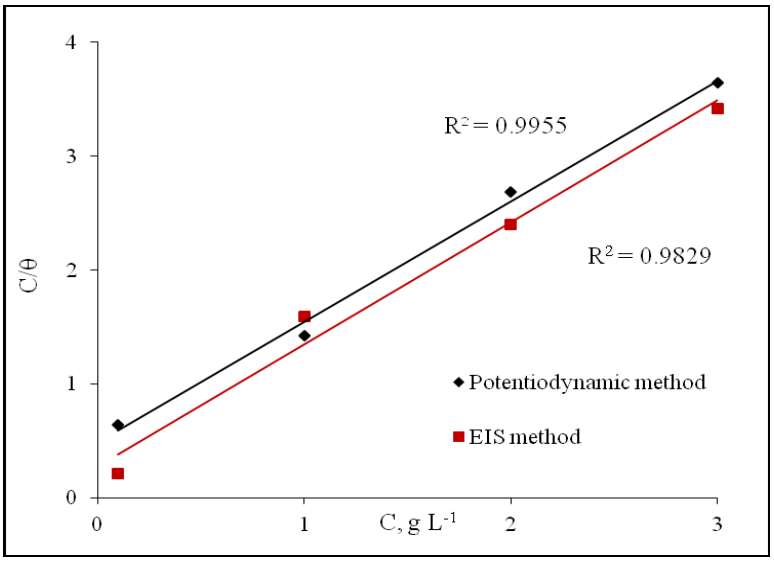

Figure 5. Langmuir isotherm adsorption model for copper with the addition of MT in 0.5 M hydrochloric acid from the potentiodynamic and EIS methods

The plots of C/θ versus C_{inh} (Figure 5) containing MT show linear lines with intercepts of K^{-1} and correlation coefficients, R^2 of 0.9955 and 0.9829 were obtained for the potentiodynamic and EIS methods, respectively. The values of $\Delta G°_{ads}$ at 303 K were obtained as -19.25 kJ mol^{-1} and -20.71 kJ mol^{-1} for the potentiodynamic and EIS methods, respectively. The linearity of the graphs confirms that the adsorption of MT follow the Langmuir isotherm model. This adsorption isotherm describes that the tannins molecules are adsorbed as a monolayer and there are no interactions with other molecules. The $\Delta G°_{ads}$ values (less than -40 $kJmol^{-1}$) obtained signify a weak spontaneous adsorption (physisorption) [34]. Hence, the tannins are physisorbed through electrostatic interactions between the inhibitor molecules and the metal surface.

3.4 SEM and EDX Studies

In order to have a better understanding of the corrosion phenomena on the copper surface, SEM analysis was carried out. The surface morphology of the copper substrate in the absence and presence of MT is shown in Figure 6 (a) and 7 (a). From Figure 6 (a), it was observed that the surface was very rough and severely damaged in the absence of inhibitor while in Figure 7 (a), the surface is transformed into smoother, more uniform deposits upon addition of MT. This is consistent with the

higher n_1 values obtained (Table 3) as compared to the blank solution. The EDX analysis of the surface in inhibitor-free solution shown in Figure 6 (b) indicated the presence of copper and chloride signals only, while the addition of MT (Figure 7 (b)) showed the presence of carbon and oxygen along with the reduction of the chloride signal. This is possibly due to the adsorption of tannin molecules via oxygen active centres of the flavanoid monomers of tannin on the metal surface [27,35]. In addition, the less porous property of the tannin covered surface as shown by the higher n_2 values (Table 3) resulted in less penetration of the chloride ions onto the metal surface.

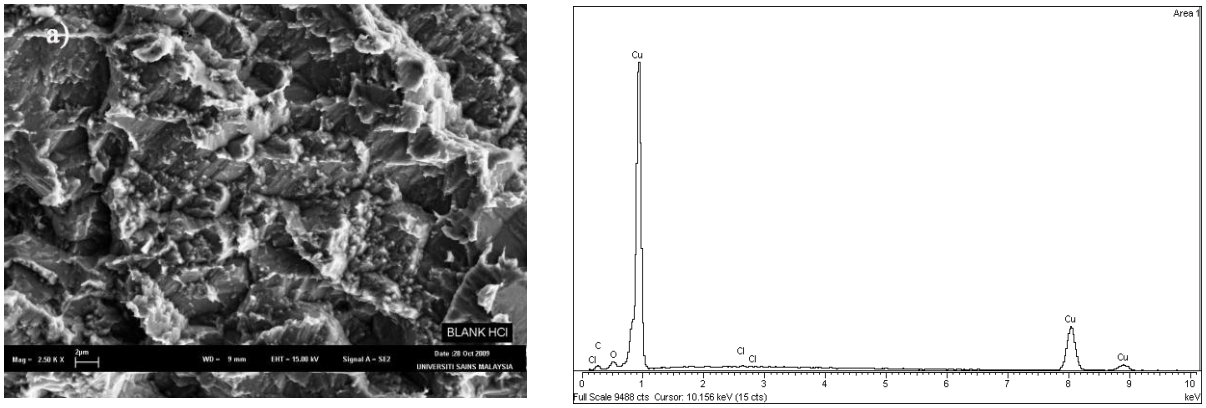

A **B**

Figure 6. (a) SEM micrograph and (b) EDX spectra of copper electrode in 0.5 M HCl

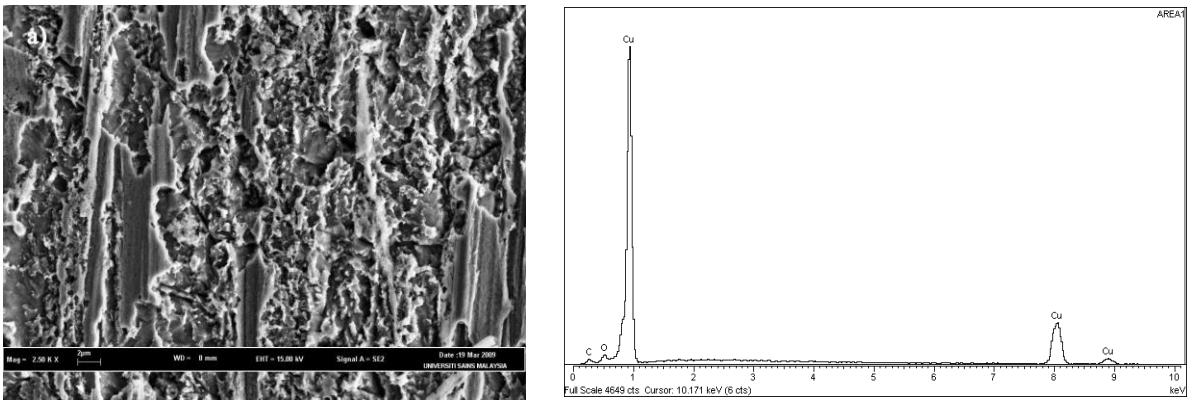

A **B**

Figure 7. (a) SEM micrograph and (b) EDX spectra of copper electrode in 0.5 M HCl in the presence of MT

3.5 Electrolyte solutions analysis

3.5.1 AAS analysis

The aim of this analysis is to determine the effect of MT concentrations on the diffusion of copper(II) ions into the electrolyte solution after gravimetric and potentiodynamic measurements. Figure 8, shows the graphs of the concentrations of copper(II) ions with increase in the concentration

of MT after gravimetric and potentiodynamic tests. Both graphs show the same trend. It was found that the concentrations of copper(II) ions decreased when the MT concentrations increased. Furthermore, the concentrations of copper(II) ions in electrolyte obtained from gravimetric test was found to be higher than the potetiodynamic measurement because of the different in immersion time of copper plate into the electrolyte solution. Generally corrosion process at the interface can be devided into two steps: (i) the oxidation of the metal (charge transfer process), and (ii) the diffusion of the metal ions from the metal surface into the electrolyte solution (mass transport process) [21]. This can thus explain the downward trend of concentrations of copper(II) ions as the MT concentrations increased. Based on this trend it can be proposed that the MT was adsorbed onto the electrode surface that resulted in the resistance of copper ions to diffuse into the electrolyte solution.

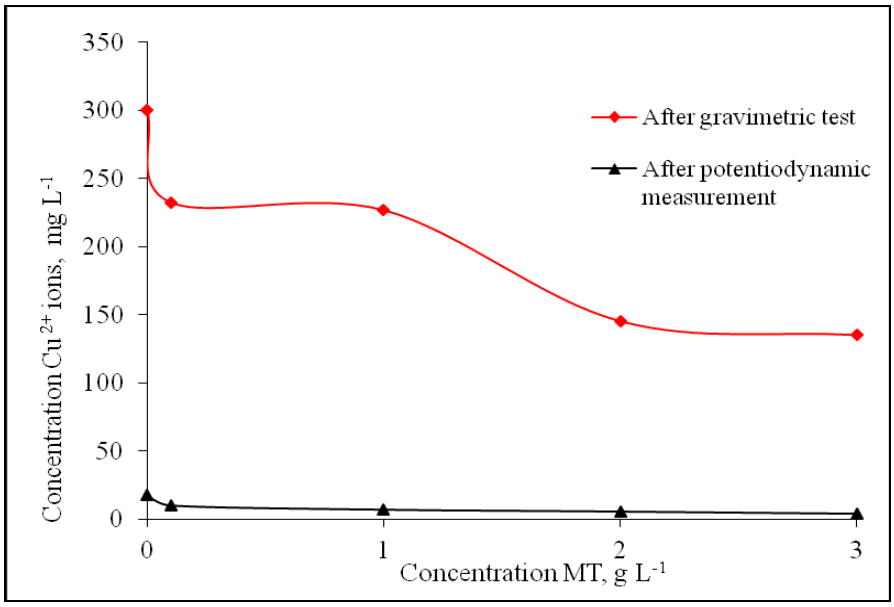

Figure 8. Graphs of the concentrations of copper(II) ions in 0.5 M hydrochloric acid after potentiodynamic and gravimetric measurements

3.5.2 IC analysis

IC analysis has been used to determine the effect of the presence of MT on the chloride concentration in the electrolyte solution after gravimetric and potentiodynamic measurements. In the blank solution (without MT), it was observed that the chloride concentration in the electrolyte after the corrosion process was low, this phenomenon is due to the adsorption of chloride ions onto the copper surface. Figure 9, shows the graphs of the chloride concentration with the increase of MT concentrations after gravimetric and potentiodynamic measurements. Both graphs show similar increase of chloride concentration with the increase in MT concentration. This observation indicated that the presence of MT increased the concentrations of chloride in the electrolyte solution by replacing the adsorbed chloride on the copper surface since the MT constituents may be adsorbed as protonated species and/or as molecular species (non-protonated). Even though the chloride present in

the blank solution have the tendency to be specifically adsorbed on the metal surface, they may also facilitate the adsorption of protonated inhibitor species by forming intermediate bridges between the metal surface and the inhibitor [36]. From the IC analysis, it also can be proposed that the presence of MT molecules in the solution may indirectly act as a physical barrier or act as a competitor to chloride to be adsorbed onto the copper surface. This is also supported by the results of EDX analysis as shown in Figure 7 (b), where the intensity of the chloride atom signals decreased in the presence of MT.

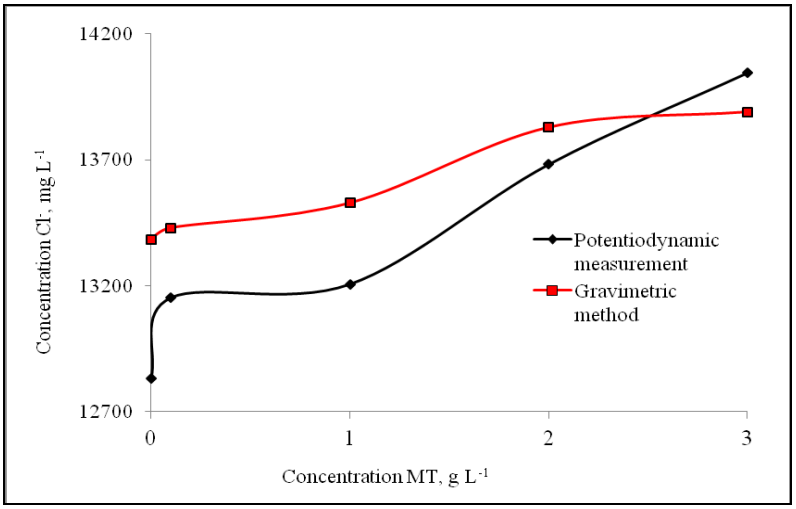

Figure 9. Graphs of the chloride concentration in 0.5 M hydrochloric acid after potentiodynamic and gravimetric measurements

4. CONCLUSIONS

Mangrove tannins behaved predominantly as cathodic inhibitors for copper corrosion in 0.5 M hydrochloric acid due to oxygen active centre properties. The inhibition efficiency obtained via electrochemical measurements is in good agreement with that obtained by using the weight loss method. SEM studies show a surface transformation upon addition of mangrove tannin. The adsorption behaviour of mangrove tannin best fitted the Langmuir adsorption isotherm. The electrolyte analysis using AAS and IC show that the presence of MT reduced the diffusion of copper(II) ions and increased the chloride ions concentrations in the electrolyte solution after the corrosion process, respectively.

ACKNOWLEDGEMENTS
The authors gratefully acknowledge the financial support of this work by Short term Grant of Universiti Sains Malaysia (304/PKIMIA/6310028 and 304/PKIMIA/6311087)

References

1. M. Scendo, *Corros. Sci*., 49 (2007) 3953.
2. L. Larabi, O. Benali, S.M. Mekelleche and Y. Harek, *Appl. Surf. Sci.*, 253 (2006) 1371.

3. H. Tavakoli, T. Shahrabi and M.G. Hosseini, *Mater. Chem. Phys*., 109 (2008) 281.
4. A.Y. El-Etre, *Corros. Sci*., 40 (1998) 1845.
5. I.H. Farooqui, A. Hussain, M.A. Quarishi and P.A. Saini, *Anti-Corros., Methods Mater.*, 46 (1999) 328.
6. A.Y. El-Etre and M. Abdallah, *Corros. Sci.*, 42(2000) 731.
7. A.Y. El-Etre, *Corros. Sci.*, 43 (2001) 1031.
8. S. Martinez and I. Štern, *J. Appl. Electrochem.*, 31 (2001) 973.
9. A.Y. El-Etre, *Corros. Sci.*, 45 (2003) 2485.
10. A.Chetouani, B. Hammouti and M. Benkaddour, *Pigm. Resin Technol.*, 33 (2004) 26.
11. A.Bouyanzer and B. Hammouti, *Pigm. Resin Technol*., 33 (2004) 287.
12. J. Mabrour, M. Akssira, M. Azzi, M. Zertoubi N Saib, A Messaoudi, A Albizane and S Tahiri, *Corros. Sci.*, 46 (2004) 1833.
13. A.Y. El-Etre, M. Abdallah and Z.E. El-Tantawy, *Corros. Sci.*, 47 (2005) 385.
14. A.M. Abdel-Gaber, B.A. Abd-El-Nabey, I.M. Sidahmed, A.M. El-Zayady and M. Saadawy, *Corros. Sci.*, 48 (2006) 2765.
15. M. Bendahou, M. Benabdellah and B. Hammouti, *Pig. Resin Technol.*, 35 (2006) 95.
16. E.E. Oguzie, A.I. Onuchukwu, P.C. Okafor and E.E. Ebenso, *Pigm. Resin Technol.*, 35 (2006) 63.
17. L. Valek and S. Martinez, *Mater. Lett.*, 61 (2007) 148.
18. O.K. Abiola, N.C. Oforka, E.E. Ebenso and N.M. Nwinuka, *Anti-Corros. Methods Mater.*, 54 (2007) 219.
19. M. Behpour, S.M. Ghoreishi, M. Salavati-Niasari and B. Ebrahimi, *Mater. Chem. Phys.*, 107 (2008) 153.
20. P.C. Okafor, M.E. Ikpi, I.E. Uwah, E.E. Ebenso U.J. Ekpe and S.A. Umoren, *Corros. Sci.*, 50 (2008) 2310.
21. A.M. Abdel-Gaber, B.A. Abd-El-Nabey and M. Saadawy, *Corros. Sci.*, 51 (2009) 1038.
22. F.S. de Souza and A. Spinelli, *Corros. Sci.*, 51 (2009) 642.
23. J. Oszmianski, A. Wojdylo, E. Lamer-Zarawska and K. Swiader, *Food Chem.*, 100 (2007) 579.
24. A.A. Rahim, E. Rocca, J. Steinmetz, M.J. Kassim M.S Ibrahim and H. Osman, *Food Chem.*, 107 (2008) 200.
25. S. Martinez and I. Stern, *Chem. Biochem. Eng. Q.*, 13 (1999) 191.
26. A.A. Rahim, E. Rocca, J. Steinmetz, M.J. Kassim R. Adnan, M.S. Ibrahim, *Corros. Sci.*, 49 (2007) 402.
27. A.R.S. Ross, M.G. Ikonomoub and K.J. Orians, *Anal. Chim. Acta.*, 411 (2000) 91.
28. D.Q. Zhang, L.X. Gao and G.D. Zhou, *J. Appl. Electrochem.*, 35 (2005) 1081.
29. K.M. Ismail, *Electrochim. Acta.*, 52 (2007) 7811.
30. M.A. Amin, S.S.A. El-Rehim, E.E.F. El-Sherbini and R.S. Bayoumi, *Electrochim. Acta.*, 52 (2007) 3588.
31. A.V. Benedeti, P.T.A. Sumodjo, K. Nobe. P.L. Cabot and W.G. Proud, *Electrochim. Acta.*, 40 (1995) 2657.
32. E.M. Sherif and S.M. Park, *Electrochim. Acta.*, 51 (2006) 4665.
33. Y. Abboud, A. Abourriche, T. Saffaj, M. Berrada M. Charrouf, A. Bennamara, N. Al Himidi and H. Hannache, *Mater. Chem. Phys.*, 105 (2007) 1.
34. T. Shahrabi, H. Tavakholi and M.G. Hosseini, *Anti-Corros. Methods Mater.*, 54 (2007) 308.
35. R. Adnan, A.R. Afidah, N. Ahmad, M.H. Norfaizah and S.A. Hamid, *Int. J. Chem.*, 18 (2008) 161.
36. E.E. Oguzie, *Mater. Chem. Phys.*, 87 (2004) 212.